

1     **A PRECONDITIONING METHOD FOR THIN HIGH CONTRAST**  
2     **SCATTERING STRUCTURES**

3             JOSEF A. SIFUENTES<sup>§</sup> AND SHARI MOSKOW<sup>†</sup>

                  27 February 2017

4     We present a method to precondition the discretized Lippmann-Schwinger in-  
5     tegral equations which model time-harmonic scalar waves in the presence of a thin  
6     inhomogeneous scatterer of high contrast. The preconditioner is based on asymptotic  
7     results as the thickness of the third component direction goes to zero and requires  
8     solving a two dimensional limiting formulation of the problem at the preconditioning  
9     step.

10    **Key words.** preconditioner, Helmholtz equation, integral methods, acoustic scattering

11    **AMS subject classifications.** 65F08, 65F10, 15A018, 47A10, 47A55

12    **1. Introduction.** We consider the problem of scattering of time-harmonic scalar  
13    waves through a thin structure of high contrast in three dimensions. Such a model  
14    arises in the study of photonic band gap structures. Photonic band gap materials are  
15    designed to guide the propagation of light by blocking certain wavelengths (the band  
16    gap), while allowing others to pass freely through, facilitating information propagation  
17    in optical communication networks and in optical computing. We consider here three  
18    dimensional slab waveguides with a two dimensional photonic crystal structure. Slab  
19    materials are typically constructed with a high refraction index and are embedded in  
20    a homogenous scattering medium, typically air. See [22], [23], [9] for more on thin  
21    photonic band gap structures.

22    We assume here that the wave phenomenon is modeled by the Helmholtz equation,  
23    keeping in mind that the full Maxwell equations are needed for three dimensional  
24    phonics. We solve the Helmholtz equation by discretizing its equivalent Lippmann-  
25    Schwinger volume integral equation formulation [8]. The resulting finite dimensional  
26    linear system is large, dense, and non-Hermitian. While there are efficient matrix-  
27    vector product routines that make an iterative solver an appealing approach [4, 6,  
28    11, 10, 17, 18], spectral properties of the system often cause Krylov subspace based  
29    iterative methods to converge slowly.

30    In [16] the authors proposed an asymptotic expansion of the Lippmann-Schwinger  
31    integral equation for inhomogeneities that are simultaneously high contrast and thin  
32    in one component direction. They showed that the the solution to a two dimensional  
33    effective model and the full three dimensional problem differed by  $\mathcal{O}(h)$  as  $h \rightarrow$   
34    0, where  $h$  is the width of the inhomogeneity in the thin component direction. A  
35    natural extension of their work is to precondition the three dimensional problem  
36    using the two dimensional operator. We formulate the preconditioner so that it can  
37    be applied to three dimensional data and yet be solved with the complexity of a two  
38    dimensional problem. We describe how to do this in section 2. We then apply the  
39    asymptotic results from [16] to obtain bounds on the GMRES residual applied to

---

<sup>†</sup>Department of Mathematics, Drexel University, Korman Center 33rd and Market St., Philadel-  
phia, PA 19104 (moskow@math.drexel.edu). The research of Moskow was partially supported by  
NSF grant DMS-1411721.

<sup>§</sup>School of Mathematical and Statistical Sciences, University of Texas - Rio Grande Valley, 1201  
West University Dr, Edinburg, TX 78539-2999 (josef.sifuentes@utrgv.edu).

40 the preconditioned system in section 3. We discuss the numerical implementation in  
 41 section 4, and finally in section 5, we demonstrate its effectiveness with numerical  
 42 examples.

43 **1.1. Problem Formulation.** We consider a (potentially inhomogeneous) scat-  
 44 terer  $S \in \mathbb{R}^3$ , thin in the third component direction, and set in a homogenous host  
 45 medium such as air or some fluid. The total scattered field  $u$  is satisfies the Helmholtz  
 46 equation

$$47 \quad (1) \quad \Delta u + \kappa^2 \epsilon(\mathbf{s})u = 0 \quad \text{for all } \mathbf{s} \in \mathbb{R}^3$$

48 where the parameter  $\kappa$  is called the wave number and defined to be  $\kappa = \omega/c_0$  for  
 49 temporal frequency  $\omega$  with  $c_0$  denoting the speed of wave propagation in the host  
 50 medium. The total scattered field  $u = u^i + u^s$  is the sum of a given incident wave  
 51  $u^i$  and a scattered wave  $u^s$ . We require the scattered wave to satisfy the Sommerfeld  
 52 radiation condition, which implies there is no wave reflection at infinity [8]:

$$53 \quad (2) \quad \frac{\partial u^s}{\partial r} - i\kappa u^s = o(1/r), \quad r = \|\mathbf{s}\|.$$

54 The incident wave  $u^i$  satisfies the freespace Helmholtz equation,  $\Delta u^i + \kappa^2 u^i = 0$  for  
 55 all of  $\mathbb{R}^3$ .

We are most interested in two dimensionally periodic photonic crystal structures  
 in a three dimensional scattering thin slab, so the refractive index is assumed to be  
 constant in the thin component direction. As in [16], we assume the scatterer is of  
 the form

$$S = \Omega \times [-h/2, h/2]$$

56 and let  $s = (\mathbf{x}, z)$  for  $\mathbf{x} \in \Omega$ ,  $\Omega$  a bounded domain in  $\mathbb{R}^2$  and  $z \in [-h/2, h/2]$ . We model  
 57 the high contrast of the squared refractive index as  $\epsilon_0(\mathbf{x})/h$ , where  $h$  is the length  
 58 of the thin side, an appropriate regime for thin slab photonic band gap structures,  
 59 where  $\epsilon_0(\mathbf{x})$  models the inhomogeneous two dimensionally periodic structure. Thus  
 60 we define the squared refractive index function

$$61 \quad (3) \quad \epsilon(\mathbf{x}, z) = \begin{cases} 1 & \text{for } (\mathbf{x}, z) \notin S; \\ \frac{\epsilon_0(\mathbf{x})}{h} & \text{for } (\mathbf{x}, z) \in S, \end{cases}$$

62 so that  $\epsilon - 1$  is compactly supported on the scatterer  $S$ . If  $u = u^s + u^i$  satisfies  
 63 equations (1) and (2), then  $u$  is also a solution to the Lippmann-Schwinger volume  
 64 integral equation [8]

$$65 \quad (4) \quad u(\mathbf{s}) + \kappa^2 \int_S \left(1 - \frac{\epsilon_0(\mathbf{s}')}{h}\right) G(\mathbf{s}, \mathbf{s}')u(\mathbf{s}') ds' = u^i(\mathbf{s}),$$

66 where  $G(\mathbf{s})$  is the free space Green's function given by

$$67 \quad (5) \quad G(\mathbf{s}, \mathbf{s}') = \frac{e^{i\kappa\|\mathbf{s}-\mathbf{s}'\|}}{4\pi\|\mathbf{s}-\mathbf{s}'\|}.$$

Using that the scatterer  $S = \Omega \times [-h/2, h/2]$  and letting  $s = (\mathbf{x}, z)$  for  $\mathbf{x} \in \Omega$  and  
 $z \in [-h/2, h/2]$ , we rewrite the Lippmann-Schwinger equation (4) as

$$u(\mathbf{x}, z) + \kappa^2 \int_{\Omega} \int_{-h/2}^{h/2} \left(1 - \frac{\epsilon_0(\mathbf{x}')}{h}\right) G((\mathbf{x}, z), (\mathbf{x}', z'))u(\mathbf{x}', z') dz' d\mathbf{x}' = u^i(\mathbf{x}, z),$$

and apply the linear change of variable  $z = h\zeta$  to obtain

$$u(\mathbf{x}, \zeta) + \kappa^2 \int_{\Omega} \int_{-1/2}^{1/2} (h - \epsilon_o(\mathbf{x}')) G((\mathbf{x}, h\zeta), (\mathbf{x}', h\zeta')) u(\mathbf{x}', \zeta') dz' d\mathbf{x}' = u^i(\mathbf{x}, h\zeta).$$

68 We write this compactly as

$$69 \quad (6) \quad (I + K)u(\mathbf{x}, \zeta) = u^i(\mathbf{x}, h\zeta),$$

70 where

$$71 \quad (7) \quad (Ku)(\mathbf{x}, \zeta) := \kappa^2 \int_{\Omega} \int_{-1/2}^{1/2} (h - \epsilon_o(\mathbf{x}')) G((\mathbf{x}, h\zeta), (\mathbf{x}', h\zeta')) u(\mathbf{x}', \zeta') d\zeta' d\mathbf{x}'.$$

72 We define our rescaled domain  $\tilde{S} = \Omega \times [-1/2, 1/2]$ , and note that the above  $K$  :  
73  $L^\infty(\tilde{S}) \rightarrow L^\infty(\tilde{S})$  is compact.

74 **2. Application of the GMRES iterative method.** Consider applying the  
75 GMRES iterative method [19] to the continuous equation (6). Since the operator  
76 we are interested in is of the form  $A := I + K$ , where  $K$  is compact,  $A$  is bounded  
77 and has only a finite spectrum outside any neighborhood of one [14, pg. 421]. Thus,  
78 unlike discretizations of the Helmholtz equation (1), refining the discretizations of the  
79 Lippmann-Schwinger equation has little effect on the conditioning of the resulting  
80 linear system and therefore little effect on GMRES performance [13], [12]. Numerical  
81 experiments in [20] show that increased mesh resolution only adds high frequency  
82 eigenmodes to the spectrum, corresponding to eigenvalues of  $A$  close to one. Thus  
83 we should expect that convergence analysis of the continuous case gives insight to  
84 convergence behavior of the discretized problem, see e.g. [5, 15, 21, 24].

85 The continuous GMRES problem is the iterative minimization problem that solves  
86 at iteration  $m$ :

$$87 \quad \|r_m\| = \min_{u \in \mathcal{K}_m(A, u^i)} \|u^i - Au\|,$$

88 where  $\mathcal{K}_m(A, u^i) := \text{span}\{u^i, Au^i, A^2u^i, \dots, A^{m-1}u^i\}$  is the Krylov subspace and  $\|\cdot\|$   
89 is an appropriate operator norm. In our paper, and following the results in [16], we  
90 will use the  $L^\infty(X)$  vector norm and the operator norm it induces, where  $X$  is a  
91 compact set in  $\mathbb{R}^2$  or  $\mathbb{R}^3$  depending on context. Since the GMRES solution to the  
92 iterative minimization problem is the product of a linear combination of monomials  
93 of  $A$  and  $u^i$ , we can write the minimizer  $u_m$  as a product of a polynomial evaluated  
94 at  $A$  of degree  $m - 1$  and the incident wave  $u^i$ . Thus we can write the residual  
95  $r_m = u^i - Au_m$  as the product of a polynomial evaluated at  $A$  of degree  $m$  times  $u^i$ ,  
96 and the polynomial is equal to 1 at the origin. Then equation 8 is equivalent to

$$97 \quad \|r_m\| = \min_{p_m \in \mathcal{P}_m^0} \|p_m(A)u^i\|,$$

98 where  $\mathcal{P}_m^0$  is the set of all polynomials of degree  $m$  or less which are equal to 1 when  
99 evaluated at the origin.

100 In practice, when the GMRES method is applied to the discretized linear system,  
101 an orthogonal basis for the approximating space is generated by the Arnoldi iteration  
102 [19], therefore the cost per iteration and memory requirements grows with each  
103 iteration as one must store the basis for the growing Krylov subspace. Thus GMRES

104 is feasible if the number of iterations remain small, but may be too computationally  
 105 expensive without effective preconditioning.

106 Now we apply the asymptotic results of [16] to build an effective preconditioning  
 107 scheme. That is, rather than apply GMRES to equation (6), we solve the equivalent  
 108 problem

$$109 \quad (AA_0^{-1})(A_0u) = u^i,$$

110 where a substantially lower order polynomial in  $\mathcal{P}_m^0$  is necessary to achieve small  
 111 residual when evaluated at  $AA_0^{-1}$ , and one can solve  $A_0y = z$  relatively quickly for  
 112 an arbitrary function  $z \in C(\tilde{S})$  (here  $A_0$  will be from a two dimensional problem). In  
 113 this case, the right hand side data need not have physical meaning; in fact it is a basis  
 114 vector of the Krylov subspace of the current GMRES iteration. We point out that  
 115 the regime for which preconditioning is necessary is when  $\kappa^2(h - \varepsilon_0)$  is of sufficient  
 116 magnitude that the compact integral operator  $K$  defined in (7) is not less than one in  
 117 magnitude. Since the operator  $A$  is a compact (and thus bounded) perturbation to  
 118 the identity, if the compact perturbation is relatively small, then GMRES is expected  
 119 to converge quickly without preconditioning.

120 To build our preconditioning operator  $A_0$ , consider the two dimensional integral  
 121 equation

$$122 \quad (8) \quad (I - K_{2D})u_0(\mathbf{x}) = u^i(\mathbf{x}, 0)$$

123 where

$$124 \quad (9) \quad (K_{2D}u_0)(\mathbf{x}) := \kappa^2 \int_{\Omega} \epsilon_o(\mathbf{x}')G((\mathbf{x}, 0), (\mathbf{x}', 0))u_0(\mathbf{x}') d\mathbf{x}'.$$

125 This is the negative of the two dimensional limiting operator for (7). Note, however,  
 126 that in order to use (8) as a preconditioner, we must extend its domain to include  
 127 functions on  $\tilde{S} = \Omega \times [-1/2, 1/2]$ . Thus we define  $K_0 : C(\tilde{S}) \rightarrow C(\tilde{S})$  by

$$128 \quad (10) \quad (K_0u)(\mathbf{x}, \eta) = K_{2D} \left( \int_{-1/2}^{1/2} u(\mathbf{x}, \eta) d\eta \right)$$

129 Note that the domain of  $K_0$  contains continuous functions on the the three dimen-  
 130 sional compact set  $\tilde{S}$ , but its image contains only functions that are constant in the  $z$   
 131 direction. Then the preconditioning operator is defined to be  $A_0 := I - K_0$ . Lemma  
 132 2 of [16] shows that  $A_0$  is continuously invertible on both  $L^2(\tilde{S})$  and  $C(\tilde{S})$ .

133 **2.1. The preconditioning step.** As mentioned before, the right hand side data  
 134 for the preconditioning operator  $A_0$  has no physical interpretation, nor is it necessarily  
 135 constant in the direction of the third component. Furthermore, for such a system  
 136  $(A_0y)(s) = z(s)$ , the solution  $y(s)$  need not be constant in the third component  
 137 direction. However, this preconditioner is only useful if we can solve it as a two  
 138 dimensional problem, which of course will have much lower computational cost than  
 139 the original three dimensional problem.

This issue is quite easily dealt with; note that if  $(A_0y)(s) = z(s)$ , then

$$(K_0y)(\mathbf{s}) = y(\mathbf{s}) - z(\mathbf{s}).$$

140 This implies that  $y(\mathbf{s}) - z(\mathbf{s})$  is constant in the  $z$  direction, and therefore equal to its  
 141  $z$  average  $\int_{-1/2}^{1/2} y(\mathbf{x}, \zeta) - z(\mathbf{x}, \zeta) d\zeta$ . This gives us the equation

$$142 \quad \kappa^2 \int_{\Omega} \int_{-1/2}^{1/2} \epsilon(\mathbf{x}')G((\mathbf{x}, 0), (\mathbf{x}', 0))y(\mathbf{x}', \zeta') d\zeta' d\mathbf{x}' = \int_{-1/2}^{1/2} y(\mathbf{x}, \zeta') - z(\mathbf{x}, \zeta') d\zeta',$$

143 which can be rearranged to be

$$144 \int_{-1/2}^{1/2} y(\mathbf{x}, \zeta') d\zeta' - \kappa^2 \int_{\Omega} \epsilon(\mathbf{x}') G((\mathbf{x}, 0), (\mathbf{x}', 0)) \left( \int_{-1/2}^{1/2} y(\mathbf{x}', \zeta') d\zeta' \right) d\mathbf{x}' = \int_{-1/2}^{1/2} z(\mathbf{x}, \zeta') d\zeta'$$

Define

$$y_a(\mathbf{x}) = \int_{-1/2}^{1/2} y(\mathbf{x}, \zeta') d\zeta'$$

and

$$z_a(\mathbf{x}) = \int_{-1/2}^{1/2} z(\mathbf{x}, \zeta') d\zeta'.$$

Then the preconditioning step is equivalent to solving the two dimension integral equation

$$y_a(\mathbf{x}) - \kappa^2 \int_{\Omega} \epsilon(\mathbf{x}') G((\mathbf{x}, 0), (\mathbf{x}', 0)) y_a(\mathbf{x}') d\mathbf{x}' = z_a(\mathbf{x}).$$

145 Given our solution  $y_a(\mathbf{x})$  to the above, we obtain our desired solution by setting

$$146 \quad y(\mathbf{x}, \zeta) = \kappa^2 \int_{\Omega} \epsilon(\mathbf{x}') G((\mathbf{x}, 0), (\mathbf{x}', 0)) y_a(\mathbf{x}') d\mathbf{x}' + z(\mathbf{x}, \zeta)$$

$$147 \quad = y_a(\mathbf{x}) - z_a(\mathbf{x}) + z(\mathbf{x}, \zeta).$$

148 That is, the  $z$  direction variations in the right hand side are simply added back into  
149 the two dimensional solutions.

150 **3. Asymptotic Results.** We present here the main result from [16] and extend  
151 it to obtain GMRES convergence bounds when applied to equations (8) and (9).

152 **THEOREM 1.** *There exists a constant  $C$ , independant of the scattering obstacle*  
153 *thickness  $h$ , such that*

$$154 \quad \sup_{(\mathbf{x}, \zeta) \in \tilde{S}} \int_{\Omega} |G((\mathbf{x}, 0), (\mathbf{x}', 0)) - G((\mathbf{x}, h\zeta), (\mathbf{x}', h\zeta'))| d\mathbf{x}' < Ch$$

155

156 *Proof.* See [16, Lemma 1]

157 It's follows from Lemma 1 of [16], that the constant  $C = \kappa M + 1$ , and  $M =$   
158  $\sup_{\mathbf{x} \in \Omega} \int_{\Omega} \|\mathbf{x} - \mathbf{x}'\|^{-1} d\mathbf{x}'$ . We can bound  $M \leq \pi d$ , where  $d = \text{diam}(\Omega)$ . This will prove  
159 to be useful in computing convergence estimates for the preconditioned scattering  
160 problem.

161 **COROLLARY 2.** *Let  $A = I + K$ , where the operator  $K$  is defined in (7) and*  
162  *$A_0 = I - K_0$ , where  $K_0$  is defined in (10). There exists a constant  $C'$ , independent*  
163 *of  $h$ , but depending on  $\kappa$  such that*

$$164 \quad \|I - AA_0^{-1}\|_{L^\infty(\tilde{S})} < C'h$$

165

*Proof.*

$$166 \quad \|I - AA_0^{-1}\| = \|(A_0 - A)A_0^{-1}\|$$

$$167 \quad \leq \|A_0^{-1}\| \|A_0 - A\|$$

168 Note that  $\|A_0^{-1}\|$  is independent of  $h$ . Consider then the asymptotic term  $\|A_0 - A\|$ .

$$169 \quad \|A - A_0\| = \sup_{\|u\|=1} \|A_0 u - Au\|$$

$$170 \quad = \sup_{\|u\|=1} \|K_0 u + Ku\|$$

171 which can be bounded to obtain  
172

$$173 \quad (11) \quad \|A - A_0\| \leq \sup_{\|u\|=1} \sup_{(\mathbf{x}, \zeta) \in \tilde{S}} \left( h\kappa^2 \int_{-1/2}^{1/2} \int_{\Omega} |G((\mathbf{x}, 0), (\mathbf{x}', 0))| |u(s')| ds' \right.$$

$$174 \quad \left. + h\kappa^2 \int_{-1/2}^{1/2} \int_{\Omega} |G((\mathbf{x}, 0), (\mathbf{x}', 0)) - G((\mathbf{x}, h\zeta), (\mathbf{x}', h\zeta'))| |u(\mathbf{x}', \zeta')| d\zeta' d\mathbf{x}' \right.$$

$$175 \quad \left. + \kappa^2 \int_{-1/2}^{1/2} \int_{\Omega} \epsilon_0(\mathbf{x}') |G((\mathbf{x}, 0), (\mathbf{x}', 0)) - G((\mathbf{x}, h\zeta), (\mathbf{x}', h\zeta'))| |u(\mathbf{x}', \zeta')| d\zeta' d\mathbf{x}' \right)$$

$$176 \quad \leq h\kappa^2 \left( \frac{M}{4\pi} + Ch + C\|\epsilon_0\|_{L^\infty(\Omega)} \right).$$

177  
178  
179 Therefore,  $\|I - AA_0^{-1}\|$  is small if the scattering medium is sufficiently thin. Note  
180 that this bound depends on the constant  $\|A_0^{-1}\|$ , which, while independent of  $h$ ,  
181 could possibly be very large. However, in practice we see that  $\|\mathbf{I} - \mathbf{A}\mathbf{A}_0^{-1}\|$  is much  
182 smaller than the bounds above, where  $\mathbf{A}$ , and  $\mathbf{A}_0$  are discretizations of  $A$  and  $A_0$   
183 respectively. The discretized operators are obtained by using a collocation method,  
184 which we describe in section 4. We plot the computed values of  $\|\mathbf{I} - \mathbf{A}\mathbf{A}_0^{-1}\|$  in Figure  
185 1.

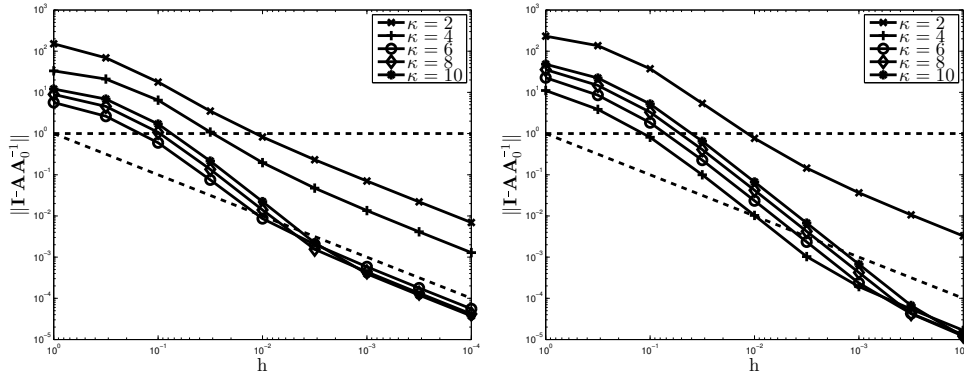


FIG. 1.  $\|\mathbf{I} - \mathbf{A}\mathbf{A}_0^{-1}\|$  for  $\epsilon_0 = 3$  on left,  $\epsilon_0 = 9$  on right.

186 The reason the results are better than the above estimate is that by factoring out  
187 the inverse of the preconditioning operator  $A_0$ , we didn't take into account spectral  
188 deflating. We show in Corollary 3 that  $\sigma(A) \in \sigma_\epsilon(A_0)$ , for  $\epsilon = O(h)$ . Thus, the  
189 spectrum of  $A_0$  approximates the spectrum of  $A$ . The numerical results in Figure 1  
190 suggest that we not only approximate well the eigenvalues, but also those eigenmodes  
191 with low enough frequency that they have small dependence on the thin direction  
192 component (of course the eigenfunctions of  $A_0$  are constant in the thin direction).  
193 Indeed we demonstrate that  $\sigma(\mathbf{A}\mathbf{A}_0^{-1}) \rightarrow 1$  as  $h \rightarrow 0$  in Figure 2.

194 COROLLARY 3. Let  $A = I + K$ , where the operator  $K$  is defined in (7) and  
 195  $A_0 = I - K_0$ , where  $K_0$  is defined in (10), then  $\sigma(A) \in \sigma_\epsilon(A_0)$ , where  $\epsilon = O(h)$ .  
 196

197 *Proof.* Let  $(\lambda, v_0)$  be an eigenpair of  $A_0$ , such that  $\|v_0\|_{L^\infty(\Omega)} = 1$ . Then

$$\begin{aligned}
 198 \quad \|(\lambda - A)v_0\|_{L^\infty(\bar{S})} &= \left| \sup_{(\mathbf{x}, \zeta) \in \bar{S}} \kappa^2 h \int_{\bar{S}} G((\mathbf{x}, h\zeta), (\mathbf{x}', h\zeta')) v_0(\mathbf{x}') d\zeta' d\mathbf{x}' \right. \\
 199 &\quad \left. + \kappa^2 \int_{\Omega} \int_{-1/2}^{1/2} \epsilon_0(\mathbf{x}') (G((\mathbf{x}, 0), (\mathbf{x}', 0)) - G((\mathbf{x}, h\zeta), (\mathbf{x}', h\zeta'))) v_0(\mathbf{x}') d\zeta' d\mathbf{x}' \right| \\
 200 &\leq h \sup_{(\mathbf{x}, \zeta) \in \bar{S}} \left| \kappa^2 \int_{\bar{S}} G((\mathbf{x}, h\zeta), (\mathbf{x}', h\zeta')) v_0(\mathbf{x}') d\zeta' d\mathbf{x}' \right| \\
 201 &\quad + \sup_{(\mathbf{x}, \zeta) \in \bar{S}} \kappa^2 \int_{\Omega} |\epsilon_0(\mathbf{x}')| |v_0(\mathbf{x}')| \int_{-1/2}^{1/2} |G((\mathbf{x}, 0), (\mathbf{x}', 0)) - G((\mathbf{x}, h\zeta), (\mathbf{x}', h\zeta'))| d\zeta' d\mathbf{x}' \\
 202 &\leq h \|K(\epsilon_0 = 1)\|_{L^\infty(\bar{S})} + Ch \|\epsilon_0\|_{L^\infty(\Omega)},
 \end{aligned}$$

203 where  $C$  is the constant from theorem 1.

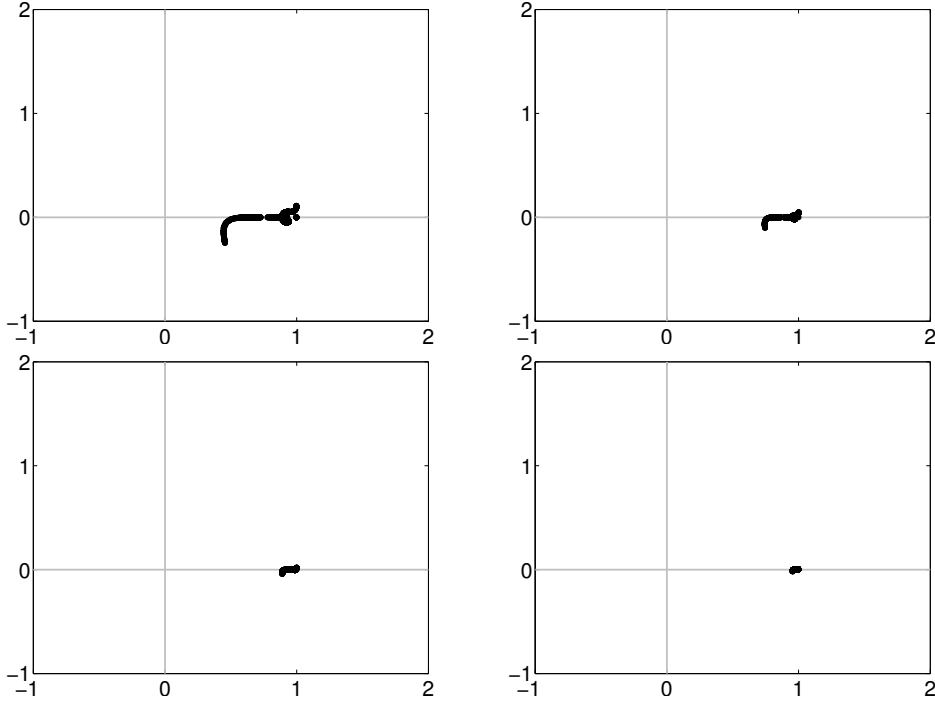


FIG. 2. The spectrum  $\sigma(\mathbf{A}\mathbf{A}_0^{-1})$  for values of  $h = 10^{-1}, 10^{-1.2}, 10^{-1.4}, 10^{-1.6}$  going left to right, top to bottom.

204 Now we can develop a bound for the preconditioned GMRES scheme.

205 COROLLARY 4. Let  $A = I + K$ , where the operator  $K$  is defined in (7) and  
 206  $A_0 = I - K_0$ , where  $K_0$  is defined in (10). Then the relative residual of the GMRES

207 *problem applied to the right preconditioned problem*

$$208 \quad (AA_0^{-1})(A_0u) = u^i,$$

209 *is bounded by  $\epsilon^m$  at each iteration  $m$ , where  $\epsilon = O(h)$ .*

210 *Proof.* Recall that we can bound the GMRES residual by the minimum of all  
211 polynomials in  $\mathcal{P}_m^0$  evaluated at  $AA_0^{-1}$ ,

$$212 \quad \|r_m\| \leq \min_{p_m \in \mathcal{P}_m^0} \|p_m(A)u^i\|.$$

213 In particular we can take  $p_m(x) = (1-x)^m$ , and use Corollary 2 to obtain

$$214 \quad \frac{\|r_m\|}{\|u^i\|} \leq \|(I - AA_0^{-1})^m\|$$

$$215 \quad \leq \|I - AA_0^{-1}\|^m$$

$$216 \quad \leq \epsilon^m$$

217 where  $\epsilon = O(h)$ .

218 **4. Numerical Implementation.** Recall that we denote the rescaled slab by  
219  $\tilde{S} := \Omega \times [-1/2, 1/2]$ . For a function  $f$  defined on  $S = \Omega \times [-h/2, h/2]$  on  $S$ , we denote  
220 by  $\tilde{f} : \tilde{S} \rightarrow \mathbb{C}$  the scaled function  $\tilde{f}(\mathbf{s}) := \tilde{f}((\mathbf{x}, \zeta)) := f((\mathbf{x}, h\zeta))$  for  $\mathbf{s} \equiv (\mathbf{x}, \zeta) \in \tilde{S}$ .  
221 That is,

$$222 \quad \tilde{G}(\mathbf{s}, \mathbf{s}') := \tilde{G}((\mathbf{x}, \zeta), (\mathbf{x}, \zeta)') := G((\mathbf{x}, h\zeta), (\mathbf{x}, h\zeta)'),$$

$$223 \quad \tilde{u}^i(\mathbf{s}) := \tilde{u}^i((\mathbf{x}, \zeta)) := u^i((\mathbf{x}, h\zeta)).$$

224 We use  $f_0 : \tilde{S} \rightarrow \mathbb{C}$  to denote functions that are constant in the  $z$  direction, that is,  
225 if  $f : \tilde{S} \rightarrow \mathbb{C}$ , then  $f_0(\mathbf{s}) := f(\mathbf{x}, 0)$ . That is,

$$226 \quad G_0(\mathbf{s}, \mathbf{s}') := G((\mathbf{x}, 0), (\mathbf{x}', 0))$$

$$227 \quad u_0^i(\mathbf{s}) := u^i((\mathbf{x}, 0)).$$

228 We discretize our shifted compact operators  $A = I + K$ , and  $A_0 = I - K_0$   
229 using a collocation method. That is, we restrict our solution space for (6) to a finite  
230 dimensional subspace, and enforce equality at a finite set of collocation points. To  
231 this end, let  $\{\phi_i\}_{i=1}^N$  be a set of linear independent functions corresponding to a  
232 discretization of our rescaled scattering obstacle  $\tilde{S}$  into the volumes  $\{d_i\}_{i=1}^N$  where  
233 the points  $\{\mathbf{s}_i\}_{i=1}^N = \{(\mathbf{x}, \xi)_i\}_{i=1}^N$  are midpoints of the discretization volumes.

234 Here we use piecewise constant basis functions  $\phi_j$  ( $\phi_j(x) = 1$  if  $x \in d_j$ , and  
235 zero otherwise) and solve for  $\tilde{u} \in \text{span}\{\phi_i\}_{i=1}^N$  by requiring equality at the collocation  
236 points  $\mathbf{s}_i$  for  $i = 1, \dots, N$ . This gives the linear system

$$237 \quad (\mathbf{I} - \mathbf{K})\mathbf{u} = \mathbf{u}^i$$

238

239 where

$$240 \quad \mathbf{K}_{ij} = \kappa^2 \int_{d_j} (h - \epsilon(\mathbf{s}')) \tilde{G}(\mathbf{s}_i, \mathbf{s}') ds'$$

$$241 \quad \mathbf{u}_i^i = \tilde{u}^i(\mathbf{s}_i)$$

242 We evaluate each entry  $\mathbf{K}_{ij}$  using a Clenshaw-Curtis quadrature scheme [7].



243 **4.1. Solving the preconditioned system.** Applying the same collocation  
 244 method to the preconditioner operator  $A_0 = I - K_0$ , we get a preconditioning matrix

245 
$$\mathbf{I} - \mathbf{K}_0$$

246 where

247 
$$(\mathbf{K}_0)_{ij} = \kappa^2 \int_{d_j} \epsilon(\mathbf{s}') G_0(\mathbf{s}_i, \mathbf{s}') d\mathbf{s}'$$

248 Note that the integral defining  $(\mathbf{K}_0)_{ij}$  integrates over the  $\Omega$  and  $z$  direction, however  
 249 the integrand is constant in the  $z$  direction. Therefore the matrix will have the tiled  
 250 structure

251 (12) 
$$\mathbf{K}_0 = d_z \begin{bmatrix} \mathbf{K}_{2D} & \mathbf{K}_{2D} & \cdots & \mathbf{K}_{2D} \\ \vdots & \ddots & & \\ \vdots & & \ddots & \\ \mathbf{K}_{2D} & \mathbf{K}_{2D} & \cdots & \mathbf{K}_{2D} \end{bmatrix},$$

where  $\mathbf{K}_{2D}$  corresponds to the discretization of the integral operator

$$(K_{2D}u)(\mathbf{x}) = \kappa^2 \int_{\Omega} \epsilon_0(\mathbf{x}') G_0(\mathbf{x}, \mathbf{x}') u(\mathbf{x}') d\mathbf{x}',$$

and  $d_z$  is the height of the discretization volumes. Thus

$$(\mathbf{K}_{2D})_{ij} = \kappa^2 \int_{\omega_j} \epsilon_0(\mathbf{x}') G((\mathbf{x}_i, 0), (\mathbf{x}', 0)) d\mathbf{x}',$$

252 where  $\{\omega_j\}_{j=1}^n$  is a discretization of  $\Omega$  corresponding to the discretization of  $\Omega \times$   
 253  $[-1/2, 1/2]$  into  $\{d_j\}_{j=1}^n$ . The entries of  $\mathbf{K}_{2D}$  are approximated using Clenshaw Curtis  
 254 quadrature.

As an analog to the continuous case, we take advantage of the tiled structure of  $\mathbf{K}_0$  to reduce the complexity. The preconditioning step involves solving, for arbitrary data  $\mathbf{z}$

$$\mathbf{y}_k - \frac{1}{m} \mathbf{K}_{2D} \sum_{i=1}^m \mathbf{y}_i = \mathbf{z}_k \quad \text{for } k = 1, \dots, m$$

where  $m$  is the number of discretizations in the  $z$  direction. Note that for our regular discretization,  $d_z = 1/m$ . Then, as a discrete analog of averaging in the  $z$  direction, we rewrite the above set of matrix equations to get

$$\frac{1}{m} \sum_{k=1}^m \mathbf{y}_k - \frac{1}{m} \mathbf{K}_{2D} \sum_{i=1}^m \mathbf{y}_i = \frac{1}{m} \sum_{k=1}^m \mathbf{z}_k.$$

Let

$$\mathbf{y}_a = \frac{1}{m} \sum_{k=1}^m \mathbf{y}_k,$$

and

$$\mathbf{z}_a = \frac{1}{m} \sum_{k=1}^m \mathbf{z}_k.$$

This yields the matrix equation on the individual blocks

$$(\mathbf{I} - \mathbf{K}_{2D})\mathbf{y}_a = \mathbf{z}_a,$$

255 from which we then reconstruct each  $\mathbf{y}_k$  from the solution to this system by

$$\begin{aligned} 256 \quad \mathbf{y}_k &= \mathbf{z}_k + \mathbf{K}_{2D}\mathbf{u}_a \\ 257 \quad &= \mathbf{z}_k - \mathbf{z}_a + \mathbf{y}_a \end{aligned}$$

258 This implies that  $\mathbf{A}_0^{-1} = (1/m)\mathbf{E} \otimes (\mathbf{A}_{2D}^{-1} - \mathbf{I}) + \mathbf{I}$ , where  $\mathbf{A}_{2D} = \mathbf{I} - \mathbf{K}_{2D}$ ,  $\mathbf{E}$  is the  
259  $m \times m$  matrix of all ones, and  $\otimes$  is the Kronecker product.

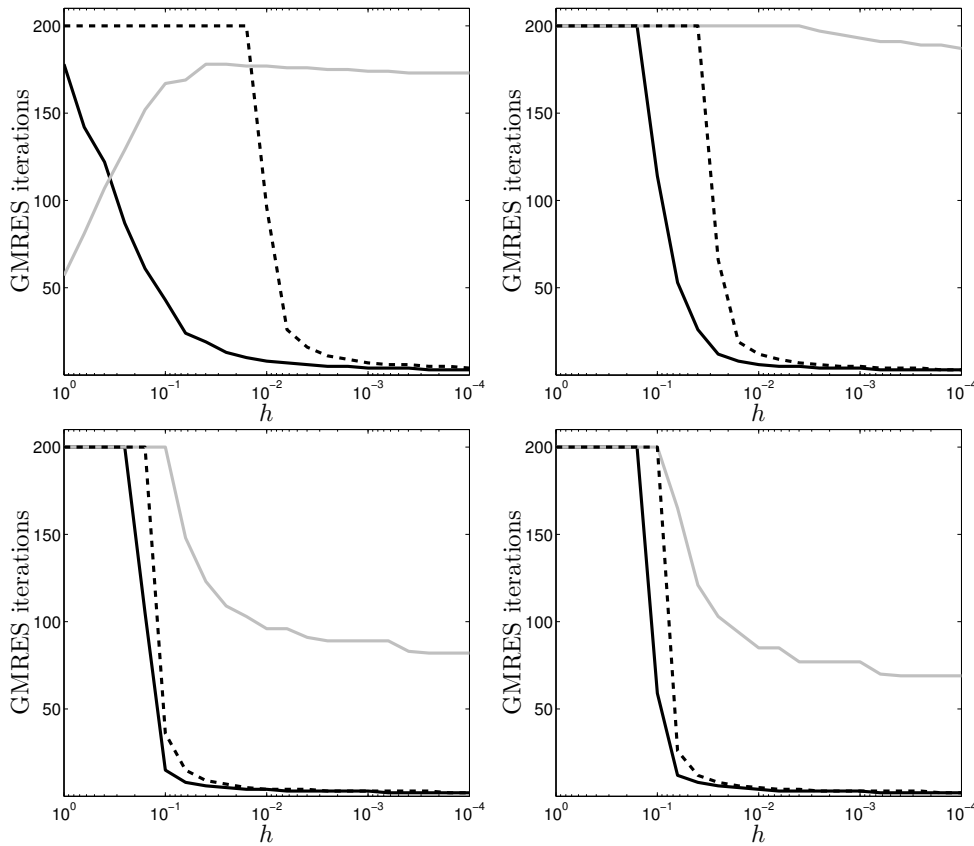


FIG. 3. GMRES Iteration counts as a function of  $h$  for  $k = 2, 4, 6, 8$  (left to right, top to bottom). The solid black line gives the iteration count for the preconditioned system. The solid grey line gives the iteration count for the unpreconditioned system. The maximum iteration was set to 200. The dashed line gives the iteration bound  $\lceil \log_\varepsilon(10^{-8}) \rceil$  if the bound is less than 200 and  $\varepsilon := \|\mathbf{I} - \mathbf{A}\mathbf{A}_0^{-1}\|_2 < 1$ . For this problem  $\varepsilon_0 = 3$  and the right hand side vector was randomly generated by Matlabs `randn` function.

260 **5. Numerical Results.** To demonstrate the effectiveness of the preconditioning  
261 scheme presented in the previous section, here we present the results of several  
262 numerical experiments. For all of the examples in this section, the scattering obstacle  
263 is a square cylinder with height  $h$ , and the grid used for discretization is  $24 \times 24 \times 7$ .

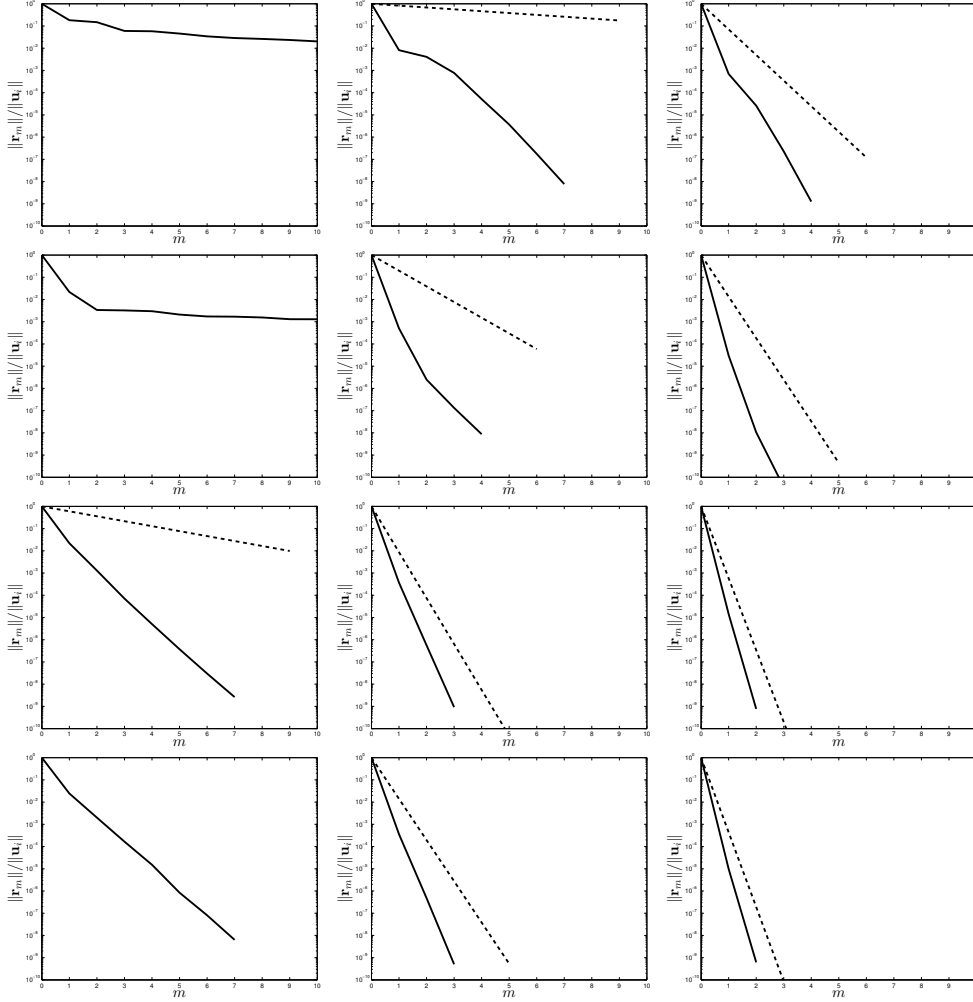


FIG. 4. For  $\kappa = 2, 4, 6, 8$  top to bottom and  $h = 10^{-1}, 10^{-2}, 10^{-3}$  left to right, we plot the first 10 relative residuals and in the solid black line and, if applicable, the bound  $\|\mathbf{I} - \mathbf{A}\mathbf{A}_0^{-1}\|_2^m$  in a dashed line. For this problem  $\epsilon_0 = 3$  and the right hand side vector is a discretization of a plane wave of wave number  $\kappa$  traveling in the  $x$  direction.

264 GMRES shows considerable improved performance when applied to the preconditioned system compared to the original discretized system for sufficiently thin inhomogeneities. Figures 3 and 5 show that for values of  $h$  near  $10^{-1}$  (and sometimes for thicker inhomogeneities), we begin to get substantial reduction in the number of GMRES iterations required for convergence. Furthermore, the numerical experiments show that the bounds demonstrated in Corollary 4 are effective at predicting the fast convergence for the preconditioned problem. The corollary suggests that the number of iterations required for convergence can be bounded by  $\lceil \log_\epsilon(\text{tol}) \rceil$  if  $\epsilon := \|\mathbf{I} - \mathbf{A}\mathbf{A}_0^{-1}\|_2 < 1$ . In all the numerical experiments presented here, the tolerance for the relative residual is set to  $\text{tol} = 10^{-8}$ .

274 For the first set of experiments, the number of Chebyshev nodes used to compute each matrix entry is  $3^2$  for the two dimensional grid and  $3^3$  for the three dimensional

276 grid, and the refractive index is constant within the scatterer. Figure 4 illustrates the  
 277 relative residual norm for the first ten iterates of the GMRES method, as well as the  
 278 bound for the residual  $\|\mathbf{I} - \mathbf{A}\mathbf{A}_0^{-1}\|_2^m$  at each iteration  $m$  if applicable.

For our next example, the refractive index is periodic and is given by

$$\varepsilon_0(\mathbf{x}) = 1 + |\sin(3x_1) \sin(3x_2)|.$$

279 The number of Chebyshev nodes used to compute each matrix entry is  $5^2$  for the  
 280 two dimensional grid and  $5^3$  for the three dimensional grid. Figure 5 illustrates  
 281 the iterations necessary for convergence for the preconditioned and unpreconditioned  
 282 system as well as the predicted iteration bound.

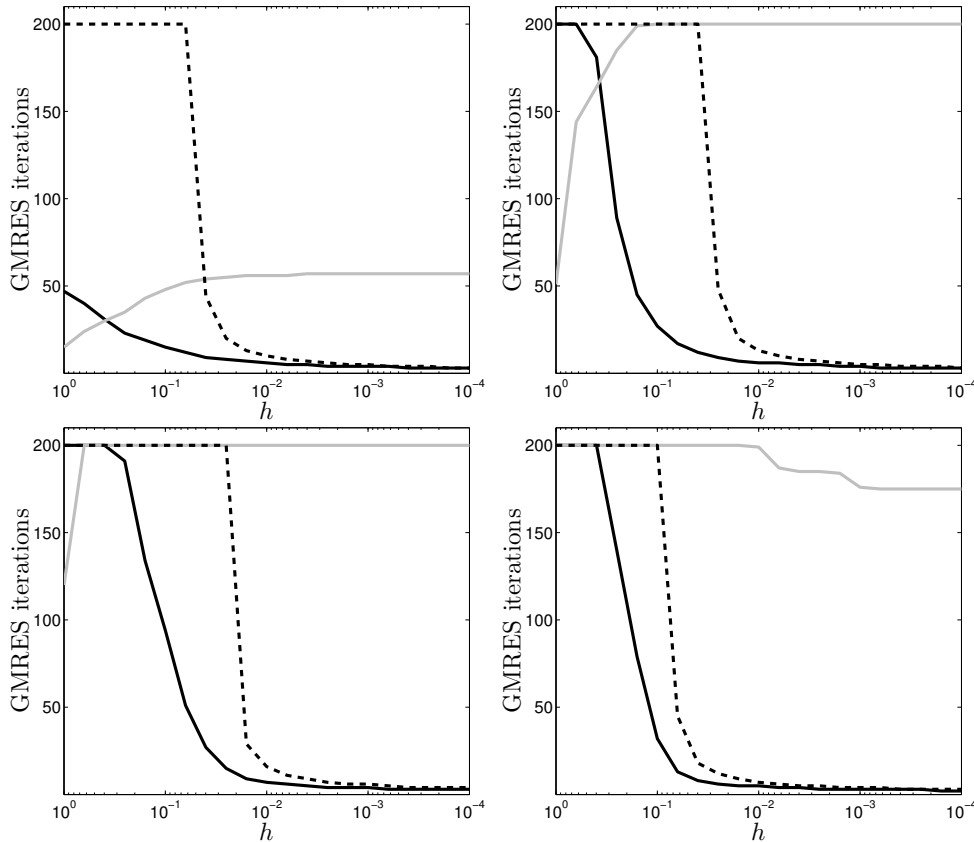


FIG. 5. GMRES Iteration counts as a function of  $h$  for  $k = 2, 4, 6, 8$  (left to right, top to bottom). The solid black line gives the iteration count for the preconditioned system. The solid grey line gives the iteration count for the unpreconditioned system. The maximum iteration was set to 200. The dashed line gives the iteration bound  $\lceil \log_\varepsilon(10^{-8}) \rceil$  if the bound is less than 200 and  $\varepsilon := \|\mathbf{I} - \mathbf{A}\mathbf{A}_0^{-1}\|_2 < 1$ . For this problem  $\varepsilon_0(x, y) = 1 + |\sin(x) \sin(y)|$  and the right hand side vector is a discretization of a plane wave of wave number  $\kappa$  traveling in the  $x$  direction.

283 **6. Conclusion and Further Work.** Analyzing thin, photonic band gap media  
 284 with two dimensional periodic structures is important for novel optical material design  
 285 [22], and the efficient computational modeling of wave propagation through such media  
 286 will be important to render three dimensional computations feasible. We have shown  
 287 that the asymptotic results in [16] can be used effectively to precondition the full

288 three dimensional scattering problem for waveguides with small thickness. Such a  
 289 preconditioner allows inner solves to be carried out in two dimensional complexity  
 290 for a three dimensional problem. We have also developed asymptotic spectral bounds  
 291 and GMRES bounds that give some indication when this preconditioning method will  
 292 be effective.

293 Similar limiting formula for thin high contrast scatterers have been obtained for  
 294 Maxwell equations [3], [2],[1], and the implementation of the analogous preconditioner  
 295 to fully resolve electromagnetic waves in three dimensions is the subject for future  
 296 work. Furthermore, thin geometry and high contrast of the inhomogeneity suggest the  
 297 use of more efficient meshes than the regular meshes used in the numerical examples  
 298 presented here. High resolution meshes will require the implementation fast integral  
 299 methods for this iterative approach to be feasible. An efficient and fast integral  
 300 algorithm would allow one to compute the matrix vector products required at each step  
 301 of the GMRES process at less than  $\mathcal{O}(N^2)$  complexity (see e.g. [4, 6, 11, 10, 17, 18]).  
 302 The examples included in this paper are low resolution and are included to illustrate  
 303 the effectiveness of the preconditioner and the sharpness of the bounds.

304

## REFERENCES

- 305 [1] D. M. AMBROSE, J. GOPALAKRISHNAN, S. MOSKOW, AND S. ROME, *Scattering of electromagnetic*  
 306 *waves by thin high contrast dielectrics ii: asymptotics of the electric field and a method*  
 307 *for inversion.* to appear *Comm. Math. Sci.*
- 308 [2] D. M. AMBROSE AND S. MOSKOW, *Scattering of electromagnetic waves by thin high contrast*  
 309 *dielectrics: effects of the object boundary*, *Commun. Math. Sci.*, 11 (2013), pp. 293–314.
- 310 [3] H. AMMARI, H. KANG, AND F. SANTOSA, *Scattering of electromagnetic waves by thin dielectric*  
 311 *planar structures.*, *SIAM J. Math. Anal.*, 38 (2006), pp. 1329–1342.
- 312 [4] O. BRUNO AND A. SEI, *A fast high-order solver for em scattering from complex penetrable*  
 313 *bodies: Te case*, *Antennas and Propagation, IEEE Transactions on*, 48 (2000), pp. 1862–  
 314 1864.
- 315 [5] Z.-H. CAO, *A note on the convergence behavior of GMRES*, *Appl. Num. Math.*, 25 (1997),  
 316 pp. 13–20.
- 317 [6] Y. CHEN, *A fast, direct algorithm for the lippmann-schwinger integral equation in two dimen-*  
 318 *sions.*, *Advances in Computational Mathematics*, 16 (2002), pp. 175–190.
- 319 [7] C. W. CLENSHAW AND A. R. CURTIS, *A method for numerical integration on an automatic*  
 320 *computer*, *Numer. Math.*, 2 (1960), pp. 197–205.
- 321 [8] D. COLTON AND R. KRESS, *Inverse Acoustic and Electromagnetic Scattering Theory*, Springer-  
 322 Verlag, Berlin, 1998.
- 323 [9] S. FAN, J. WINN, A. DEVENYI, J. CHEN, R. MEADE, AND J. JOANNOPOULOS, *Guided and defect*  
 324 *modes in periodic waveguides*, *J. Opt. Soc. Amer. B Opt. Phys.*, 12 (1995), pp. 1267–1283.
- 325 [10] L. GREENGARD AND V. ROKHLIN, *A fast algorithm for particle simulations*, *Journal of Com-*  
 326 *putational Physics*, 135 (1997), pp. 280 – 292.
- 327 [11] E. M. HYDE AND O. P. BRUNO, *An efficient, preconditioned, high-order solver for scattering*  
 328 *by two-dimensional inhomogeneous media*, *J. Comp. Phys.*, 200 (2004), pp. 670–694.
- 329 [12] ———, *A fast, higher-order solver for scattering by penetrable bodies in three dimensions*, *J.*  
 330 *Comp. Phys.*, 202 (2005), pp. 236–261.
- 331 [13] C. JOHNSON, *Numerical Solution of Partial Differential Equations by the Finite Element*  
 332 *Method*, Cambridge University Press, Sweden, 1995.
- 333 [14] E. KREYSZIG, *Introductory Functional Analysis with Applications*, Wiley, New York, 1989.
- 334 [15] I. MORET, *A note on the superlinear convergence of GMRES*, *SIAM J. Num. Anal.*, 34 (1997),  
 335 pp. 513–516.
- 336 [16] S. MOSKOW, F. SANTOSA, AND J. ZHANG, *An approximate method for scattering by thin struc-*  
 337 *tures*, *SIAM J. Appl Math.*, 66 (2005), pp. 187–205.
- 338 [17] K. NABORS, F. T. KORSMEYER, F. T. LEIGHTON, AND J. WHITE, *Preconditioned, adaptive,*  
 339 *multipole-accelerated iterative methods for three-dimensional first-kind integral equations*  
 340 *of potential theory*, *SIAM J. Sci. Comput.*, 15 (1994), pp. 713–735.
- 341 [18] V. ROKHLIN, *Rapid solution of integral equations of scattering theory in two dimensions*, *Journal*  
 342 *of Computational Physics*, 86 (1990), pp. 414 – 439.

- 343 [19] Y. SAAD AND M. H. SCHULTZ, *GMRES: A generalized minimal residual algorithm for solving*  
344 *nonsymmetric linear systems*, SIAM J. Sci. Stat. Comp., 7 (1986), pp. 856–869.
- 345 [20] J. SIFUENTES, *Preconditioning the integral formulation of the helmholtz equation via deflation*,  
346 Master’s thesis, Rice University, 2006.
- 347 [21] V. SIMONCINI AND D. B. SZYLD, *On the occurrence of superlinear convergence of exact and*  
348 *inexact Krylov subspace methods*, SIAM Review, 47 (2005), pp. 247–272.
- 349 [22] P. VILLENEUVE, S. FAN, S. JOHNSON, AND J. JOANNOPOULOS, *Three-dimensional photon con-*  
350 *finement in photonic crystals of low-dimensional periodicity*, IEE Proc. Optoelectron, 145  
351 (1998), pp. 384–390.
- 352 [23] J. VUCKOVIC, M. LONCAR, H. MABUCHI, AND A. SCHERER, *Optimization of the q factor in*  
353 *photonic crystal microwavities*, IEEE J. Quantum Elec., 38 (2002), pp. 850–856.
- 354 [24] R. WINTHER, *Some superlinear convergence results for the conjugate gradient method*, SIAM  
355 J. Num. Anal., 17 (1980), pp. 14–17.